J Clin Exp Hematop
Vol. 55, No. 3, Dec 2015

Original Article

Plasmacytoid Dendritic Cells Producing Interferon-α (IFN-α) and Inducing Mx1 Play an Important Role for $CD4^+$ Cells and $CD8^+$ Cells in Necrotizing Lymphadenitis

Hiroko Sato,[1)*] Shigeyuki Asano,[2)*] Kikuo Mori,[2)] Kazuki Yamazaki,[2)] and Haruki Wakasa[3)]

We confirmed the characteristic clinical features of necrotizing lymphadenitis (NEL) in 66 cases (23 male, 43 female) in Japan, which included high fever (38-40℃), painful cervical lymphadenopathy (62/66, 93.9%), and leukopenia (under 4,000/mm^3) (25/53, 47.2%), without seasonal occurrence, in a clinicopathological, immunohistochemical, electron microscopic serological study. Patient age varied from 3-55 years, and 72.7% (44/66) of patients were younger than 30 years. Histopathology of NEL was characterized by the presence of $CD8^+$ immunoblasts, $CD123^+$ cells (plasmacytoid dendritic cells; PDCs), histiocytes and macrophages phagocytizing $CD4^+$ apoptotic lymphocytes, but no granulocytes or bacteria. The number of PDCs and $CD8^+$ cells in lesions tended to increase with time, and PDCs tended to be larger and irregular in the lesions compared with the non-lesion tissue of the lymph nodes. In addition, PDCs showed no temporal morphological change in the lymph nodes. The number of $CD4^+$ cells in the lymph node lesions sharply decreased from the 2nd to the 4th week, and then tended to increase; however, $CD4^+$ cells gradually decreased with time in non-lesion tissue. PDCs may produce interferon-α (IFN-α), which induces Mx1 expression. Strong Mx1 immunoreactivity is indicative of IFN-α production. IFN-α induces transformation of $CD8^+$ cells into immunoblasts, as well as phagocytosis of apoptotic cells derived from $CD4^+$ cells by macrophages. Thus, PDCs may play an important role with immune cells, including $CD8^+$ and $CD4^+$ cells, in necrotizing lymphadenitis. 〔*J Clin Exp Hematop 55(3) : 127-135, 2015*〕

Keywords: necrotizing lymphadenitis, cervical lymph node, plasmacytoid dendritic cells, interferon-α, Mx1

INTRODUCTION

Necrotizing lymphadenitis (NEL), is clinically characterized by unknown fever and cervical lymphadenopathy, and is not commonly observed in oral surgery. This disease was originally reported by Japanese researchers in the early 1970s,[1-3] and has since been reported in other geographic regions.[4-9] The lymph node lesions of this disease have been extensively studied,[1-3,5-12] but to the best of our knowledge, there have been no reports in the literature describing in detail the change in distribution and morphology of plasmacytoid dendritic cells (PDCs), or the associations among $CD4^+$ cells, $CD8^+$ cells, PDCs, and peripheral blood monocytes and their time courses. Here, we investigated and discuss the role of PDCs in NEL by observing temporal changes in PDC morphology and the number of $CD123^+$ (PDCs), $Mx1^+$, $CD8^+$, and $CD4^+$ cells.

Received: August 19, 2015
Revised : October 1, 2015
Accepted: October 22, 2015
[1)]Department of Dentistry and Oral Surgery, Iwaki Kyoritsu General Hospital, Iwaki, Fukushima, Japan
[2)]Department of Pathology, Iwaki Kyoritsu General Hospital, Iwaki, Fukushima, Japan
[3)]Surgical Pathology Japan, Company Ltd., Sendai, Miyagi, Japan
Corresponding author: Shigeyuki Asano, M.D., Ph.D., Department of Pathology, Iwaki Kyoritsu General Hospital, 16 Kusehara, Mimayamachi, Uchigo, Iwaki, Fukushima, 973-8555, Japan
Email: patho.asano@gmail.com
*These authors (HS & SA) contributed equally to this work.

MATERIALS AND METHODS

The data of 66 cases performed between 1989 and 2014 at Iwaki Kyoritsu General Hospital in Japan were collected, and all associated patient files kept at the hospital were used for this study. The files of each patient included clinical data related to symptoms, onset days, biopsy day, laboratory tests, and computed tomography. The number of $CD4^+$ cells and $CD8^+$ cells, measured by flow cytometry 11 to 2,035 days after onset of the disease, were available in 8 cases (30 samples). Serological data, including antibody titer for Epstein–Barr virus (EBV) (23 samples), cytomegalovirus (6 samples), and toxoplasma (2 samples), were available in 28 cases (30 samples).

Lymph node biopsy samples were divided into three portions; one was fixed in 10% formalin for routine diagnosis, another fixed in 2.5%-glutaraldehyde for conventional elec-

tron microscopy (EM), and the third was used for imprint cytology, fixed in 95% ethyl alcohol. Sections cut from the 10%-formalin-fixed paraffin-embedded (FFPE) lymph node samples were stained with hematoxylin-eosin, Giemsa, periodic acid-Schiff, silver impregnation, and elastica-Masson. Imprint cytological specimens on glass slides were stained with Papanicolaou and Giemsa stains. For immunohistochemistry (IHC), FFPE tissue sections (4 μm thickness) were deparaffinized in xylene and rehydrated through graded alcohols and rinsed in distilled water. Antigen retrieval was performed in 0.01 M citric acid monohydrate (pH6.0) (Koso Chemical Co., Ltd., Tokyo, Japan), or at pH9.0 for CD123 (Nichirei, Tokyo, Japan), using standard microwave and autoclave heating for 15 or 20 min, respectively. IHC was performed using an automated stainer (Nichirei) according to the manufacturer's instructions, and the sections were mounted with Malinol (Muto Pure Chemicals Co., Ltd., Tokyo, Japan). The panel of antibodies used included antibodies against CD3 (Roche Diagnostics, AZ, USA), CD4, CD10, myeloperoxidase (MPO) (Nichirei), CD5, CD8, CD20, CD30, CD68, EBV-encoded small RNA (EBER), S-100 protein, Ki-67, HLA-DR (Dako, CA, USA), CD123 (BioLegend, CA, USA), CD163 (Lab Vision, CA, USA), Langerin (Novocastra, Newcastle, UK), Mx1 (Thermo scientific, IL, USA), and CD204 (Dr. Takeya, Kumamoto, Japan) (Table 1). EBER was investigated in 20 cases (20 samples) by *in situ* hybridization of FFPE tissue sections (4 μm thickness) using a DAKO Detection Kit (Dako). Sections with known reactivity to the antibodies used served as positive controls. Negative controls for IHC were obtained by omission of the primary antibody and substitution with phosphate buffer saline.

Of 18 temporally different cases, the proportion of $CD4^+$, $CD8^+$, $CD123^+$ cells (PDCs), and $Mx1^+$ cells were counted out of 400 cells per lesion and per normal portion of the same tissue section in five lesions per case, using an attached meshed eyepiece.

Statistical analysis of the temporal change of each cell and associations among the cell groups described above was performed using image analysis software (IMAGE J 1.48 v; NIH, USA), and the Mann-Whitney U test (SPSS version 11, IBM, USA) was used to investigate the morphological differences of the cytoplasm and nucleus of PDCs found in lesions and in non-lesion tissues, and changes in time of parameters including area, circularity, roundness, minor/major axis ratio, nuclear cytoplasm ratio, and perimeter. Values of $p < 0.05$ were considered significant.

For EM, lymph node specimens were fixed in 2.5% glutaraldehyde, post-fixed in 1.0% OsO_4, and embedded in Epon 812. Ultrathin sections were stained with uranyl acetate and lead citrate, and were examined using EM.

Table 1. Antibodies used in the immunohistochemical study

Antibody	Clone	Specificity	Source	Clonality	Retrieval	Dilution
CD3	2GV6	T cells	Roche	M	Mic	1:1
CD4	1F6	Helper T cells	Nichirei	M	Mic	1:1
CD5	CD5/5456	T cells	Dako	M	Mic	1:100
CD8	C8/144B	Killer T cells	Dako	M	Mic	1:1
CD10	56C6	CALLA, immature B cells, germinal center B cells	Nichirei	M	Mic	1:1
CD20	L26	B cells	Dako	M	Mic	1:1
CD30	Ber-H2	Activated B cells	Dako	M	Mic	1:100
CD68	KP1	Macrophages, plasmacytoid T cells	Dako	M	Mic	1:50
CD123	6H6	Dendritic cells, myeloid precursor cells, macrophages	Bio	M	Mic	1:100
CD163	10D6	Macrophage scavenger receptor	Lab	M	Mic	1:50
CD204		Macrophage scavenger receptor	a	M	Mic	1:1
Langerin	12D6	Langerhans cells	Novo	M	Mic	1:100
S-100 protein		Langerhans cells, melanocytes, Schwan cells	Dako	P	Non	1:1
HLA-DR	TAL. 1B5	Langerhans cells, macrophages, B cells, activated T cells	Dako	M	Mic	1:25
Ki-67	MIB1	Human proliferating cells	Dako	M	Mic	1:1
Myeloperoxidase	59A5	Granulocytes, monocytes	Nichirei	M	Mic	1:1
EBER (*in situ* hybridization)	EBV		Dako	M	Mic	1:1
Mx1	IFI-78K	Interferon-induced GPT-binding protein Mx1 (MxA)	Therm	P	Non	1:1,000

Roche, Roche Diagnostics, AZ, USA; Nichirei, Nichirei, Tokyo, Japan; Dako, Dako, CA, USA; Bio, BioLegend, CA, USA; Lab, Lab Vision, CA, USA; Novo, Novocastra, Newcastle, UK; Therm, Thermo Scientific, IL, USA; M, monoclonal; P, polyclonal; Mic, microwave; Non, non-treated

[a], Anti-CD204 antibody was supplied by Dr. Takeya, Graduate School of Medical Science, Kumamoto University, Kumamoto, Japan.

RESULTS

Clinical findings

Clinical features of the patients are shown in Fig. 1 and 2. There were 23 male and 43 female patients (M/F = 1/1.87), aged 3-55 years (average, 25.7 years; median, 26.0 years; 66.7% (44/66) younger than 30 years). The peak of disease onset was in the 20s (25/66, 37.9%) (Fig. 1). No seasonal occurrence was found. Most patients complained of dull or acutely painfully swollen cervical lymph nodes (62/66, 93.9%) (Fig. 2), frequently on the left-side (27/64, 42.2%) and right-side (21/64, 32.8%) (Fig. 3). In addition, initial tonsillar swelling (13/36, 36.1%), and transient skin rash were observed, but no hepatosplenomegaly. A skin rash similar to rubella or drug-induced eruption tended to appear in febrile and severe cases. The fever seldom responded to antibiotics, but steroid and antichloristics were effective. The period of illness was almost always limited to one attack, although 11 cases (11/66, 16.7%) recurred within 5 months-19.8 years after onset. Most recurrent cases frequently were on the left-side of the neck in females. One 47-year-old female suffered attacks three times within 7 years. In these cases, symptoms resembled those of the onset of the disease. No familial cases were recorded in the files. Almost all patients had consulted a physician for common cold-like symptoms, such as persistent high fever (38-40℃), general malaise, and painful cervical lymphadenopathy. The symptoms lasted for approximately one week, but in rare cases up to one month. In those with available peripheral white blood cell counts, 47.2% (25/

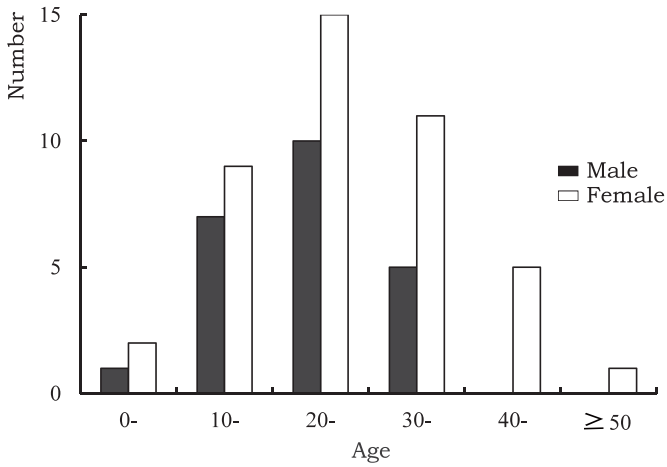

Fig. 1. Age and sex distribution of the 66 cases. The majority of patients (44/66, 66.7%) were younger than 30 years.

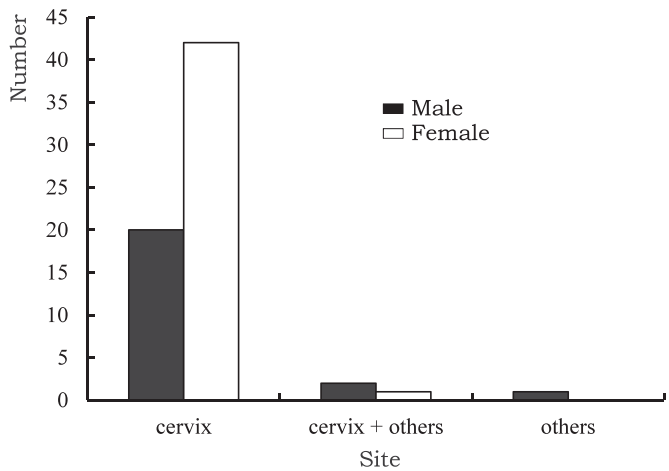

Fig. 2. Sites of affected lymph nodes of the 66 cases. Cervical lymph nodes were the most common affected site.

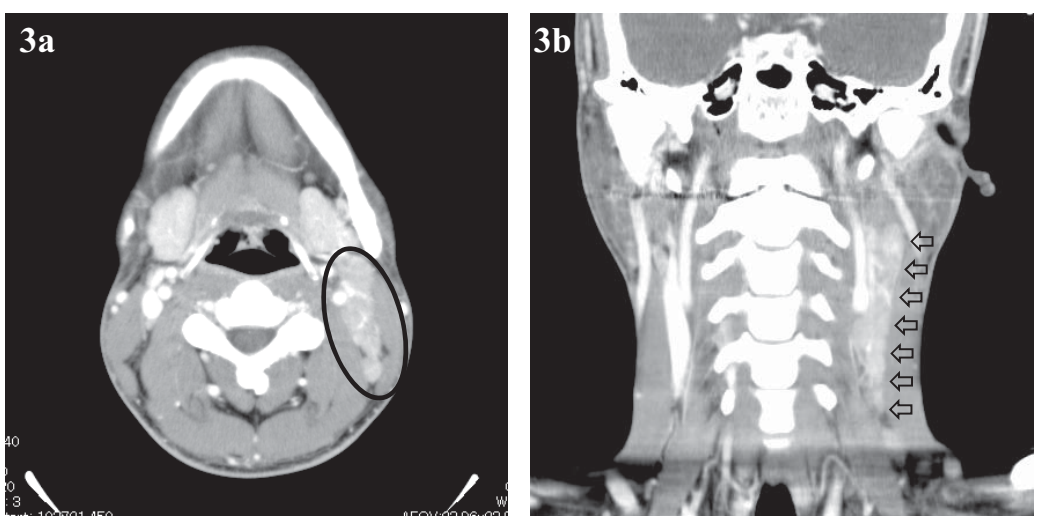

Fig. 3. Computed tomography. Swollen lymph nodes lesions are observed at the left side of the neck. 27-year-old male. (*3a*); axial section (*circle*), (*3b*); coronal section (*arrows*).

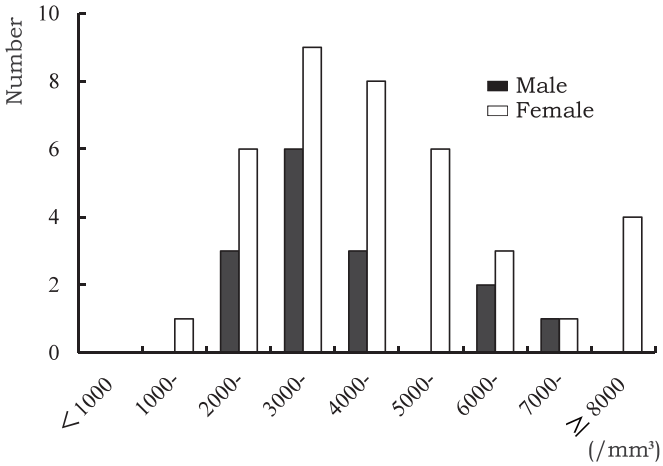

Fig. 4. White blood cells of the peripheral blood of 53 cases. White blood cell count is less than 4,000/mm^3 (25/53, 47.2%).

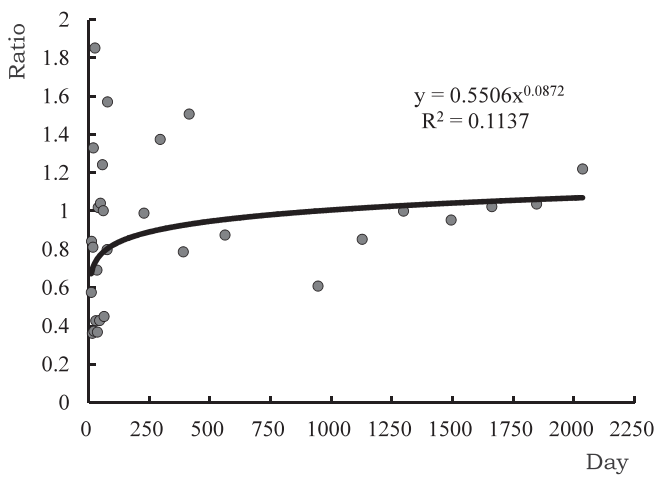

Fig. 5. CD4$^+$/CD8$^+$ cell ratio of the peripheral blood of 8 cases (30 samples). The ratio is lower than 1.0 in the early stage, but gradually approaches 1.0.

53) of patients showed a decrease count to under 4,000/mm^3 (Fig. 4). CD8$^+$ cells in peripheral blood were more abundant than CD4$^+$ cells from the onset of the disease, but CD8$^+$ cells gradually decreased through the clinical course, resulting in an increasing CD4$^+$/CD8$^+$ cell ratio (Fig. 5). In some patients, aspartate aminotransferase, alanine aminotransferase, erythrocyte sedimentation rate, and titer of anti-nuclear antibody were found elevated with an initially rapid rise, and then later returned to normal. In addition, lactate dehydrogenase, soluble interleukin 2 receptor, C-reactive protein, and ferritin remained within normal range. Peripheral blood monocytes showed increased levels in 67.3% of cases (33/49) (Fig. 6). Increased antibody titers for EBV, cytomegalovirus, and toxoplasma were not found in any detectable cases. Furthermore, whenever available, antibody titers of paired sera did not

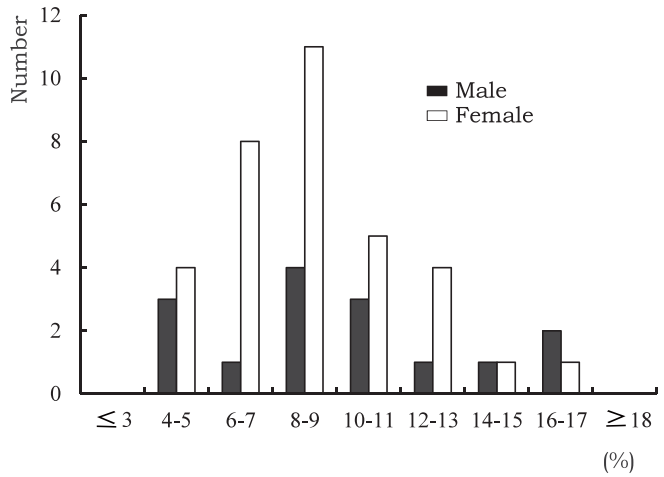

Fig. 6. Peripheral blood monocytes of 49 cases. Thirty-three cases show an abnormal count (more than 8%) of peripheral blood monocytes.

differ from one another. Although thirteen patients were admitted, there were no fatalities. No cases showed malignant transformation.

Pathological findings

Surgical biopsies or fine-needle aspiration cytology were performed from 4 to 161 days after onset. Lymph nodes were up to 2.5 cm in diameter, smooth and soft. Irregular yellowish foci were often observed on the cut surface. Several cases showed periadenitis with capsular thickening. Lesions appeared mainly in the paracortical area, where the depletion of lymphocytes was greatest (Fig. 7a). Lymph follicles remained sporadically throughout the lesion. Cytological and histological features of involved lymph nodes included the presence of immunoblasts, PDCs, histiocytes, and MPO$^+$, CD68$^+$, CD163$^+$, and CD204$^+$ macrophages, the latter with phagocytized nuclear debris derived mainly from apoptotic lymphocytes; however, no granulocytes or bacteria were found (Fig. 7b). Ki-67$^+$ cells were abundant (48.8%) in the lesions. EBER$^+$ cells detected by *in situ* hybridization were rare in the paracortical areas in affected lymph nodes. CD8$^+$ cells in the lymph nodes had large round nuclei corresponding to immunoblasts. CD4$^+$ cells in the lymph nodes had smaller nuclei, and were often apoptotic and phagocytized by macrophages. PDCs were mixed with other cells in the lesions and were often observed near the endothelium of the vessel (Fig. 8a, 8b). PDCs were about 12.7 μm in size and the nuclear cytoplasm ratio was approximately 0.4. The PDCs had round or slightly elongated nuclei with a smooth nuclear membrane. Results of the morphological analysis of the PDCs are shown in Table 2. PDCs tended to be larger and irregular in the lesions compared with those in the non-lesions tissue of the

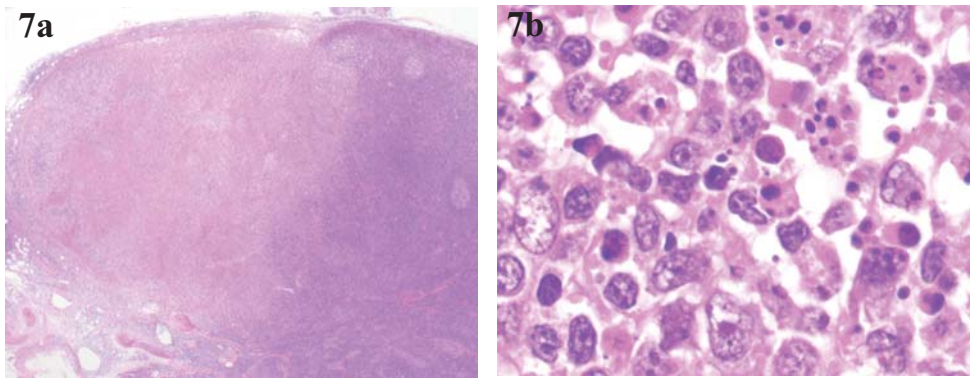

Fig. 7. Histological features of lymph node lesions. (*7a*) Pale, blurred lesion in a lymph node of necrotizing lymphadenitis. Several atrophic lymph follicles are observed on the right side. (*7b*) Immunoblasts with distinct nuclei are intermixed with small lymphocytes and macrophages that had phagocytized apoptotic lymphocytes.

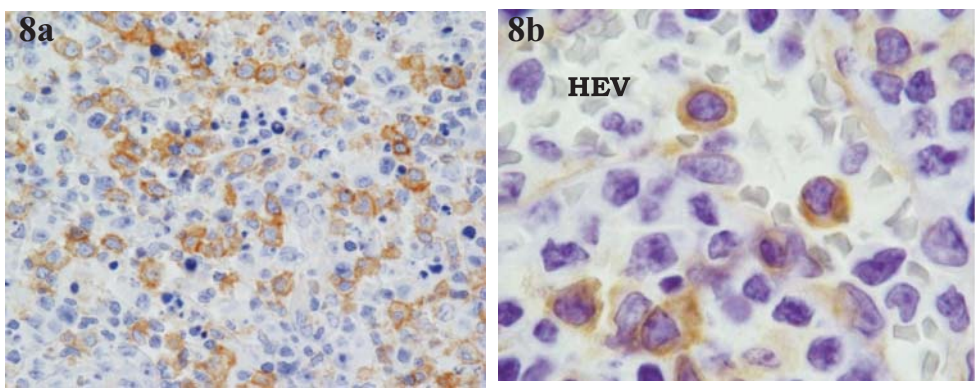

Fig. 8. $CD123^+$ cells. (*8a*) $CD123^+$ cells include plasmacytoid dendritic cells (PDCs) and are distributed through the lesions and not in non-lesion tissue. (*8b*) PDCs are observed within the high endothelial venule (*HEV*) and near the venule.

Table 2. Morphological analysis of plasmacytoid dendritic cells between those found in lesions and non-lesion tissue.

	Parameter	Lesion	Non-lesion	*p*-value (Mann-Whitney)
Cytoplasm	Area	93.93	82.01	0.01
	Circularity	0.72	0.74	0.05
	Roundness	0.72	0.71	
	Axis ratio*	1.39	1.40	
	Perimeter	40.92	37.6	0.01
Nucleus	Area	34.19	29.5	0.01
	Circularity	0.75	0.73	0.05
	Roundness	0.71	0.66	0.01
	Axis ratio*	1.41	1.51	0.05
	Perimeter	24.45	23.61	0.01
	N/C ratio**	0.37	0.38	

*, minor/major axis ratio; **, nuclear/cytoplasm ratio

lymph nodes.

By electron microscopy, PDCs showed linear chromatin located at the cell membrane, and nucleoli were often observed. Lamellar and long rough endoplasmic reticula and cytoplasmic organelles were often aggregated on one side of the cytoplasm. Although no phagocytic activity was observed, tubuloreticular structures were occasionally observed in the cytoplasm (Fig. 9, inset).

$Mx1^+$ cells included PDCs, macrophages, immunoblasts, and endothelial cells, but not small lymphocytes in the NEL lesions (Fig. 10a, 10b). $Mx1^+$ cells were more numerous in the lesions than in the accompanying non-lesion tissue, and was correlated with PDC and macrophage density.

The number of $CD8^+$ cells and PDCs in the lymph node lesions increased with time, similar to the peripheral blood monocytes; however, the number of $CD4^+$ cells in the lesions sharply decreased from the 2nd to the 4th week, and then

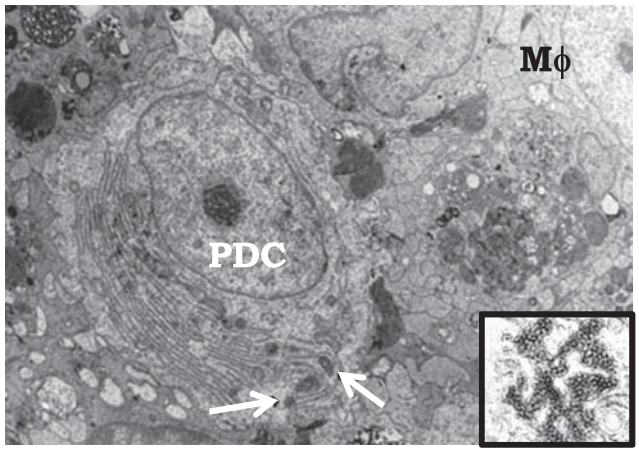

Fig. 9. Characteristic electron microscopic features of plasmacytoid dendritic cells (*PDCs*). The PDC has characteristic eccentrically-distributed nuclei and lamellar rough endoplasmic reticulum in the cytoplasm. A macrophage (*Mϕ*) phagocytizing apoptotic lymphocytes is observed near the PDC. *Arrows* show tubuloreticular structure. *Inset*; Tubuloreticular structure in the cytoplasm of the PDC, showing bead-like structures filling the endoplasmic reticulum space.

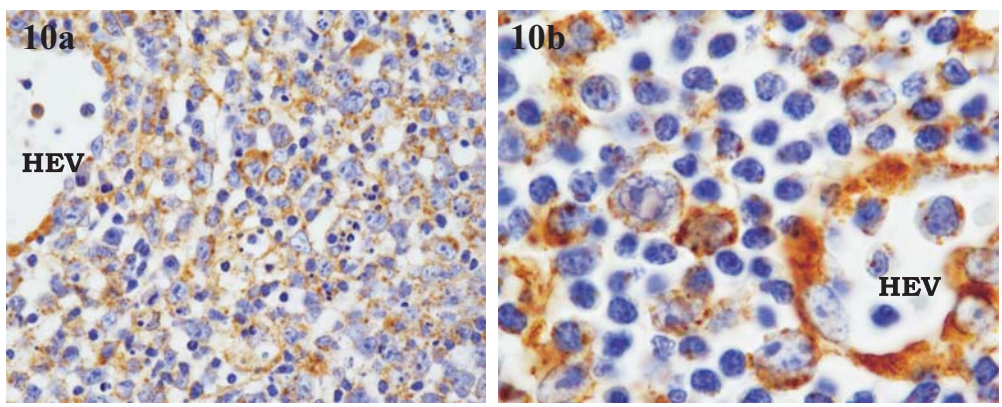

Fig. 10. $Mx1^+$ cells. (*10a*) $Mx1^+$ cells included plasmacytoid dendritic cells, macrophages, immunoblasts, and endothelial cells in the lesions. *HEV*, high endothelial venule. (*10b*) $Mx1^+$ cells are observed among lymphocytes and within the high endothelial venule (*HEV*) in non-lesions.

tended to increase afterward (Table 3) (Fig. 11A). In non-lesions, the number of $CD8^+$ cells and PDCs showed almost no changes, but the number of $CD4^+$ cells gradually decreased with time (Fig. 11B). The $CD4^+/CD8^+$ cell ratio in the lymph node lesions did not show the same correlation as was observed in the peripheral blood.

DISCUSSION

NEL is a self-limited benign disorder, and is clinically characterized at onset by common cold-like symptoms, such as fever (38-39℃), painful cervical lymphadenopathy, and leukopenia.[4,5,10,11,13] This disorder has a female predilection, with a ratio of affected males to females reported to be 1:1.3-1:1.87,[4,14] and the average onset is from the third to fourth decade. Lymphadenopathy appears mainly in the cervical regions (80.3-93.8%),[4,12,14]and leukopenia (under 4,000/mm^3) is often observed in the early stages.[3,4,14] The symptoms seldom respond to antibiotics; however, steroid, analgesic, and anti-inflammatory agents are effective.[14]

We observed that the $CD4^+/CD8^+$ cell ratio in the peripheral blood was less than 1.0 because of marked decrease of $CD4^+$ cells due to apoptosis in the lymph nodes from the 2nd to 4th week. Thus the conditions observed in the peripheral blood may reflect those of the affected lymph nodes.[4,14-16] We propose that $CD8^+$ cells may be activated by some etiology, such as virus infection, resulting in transformation into immunoblasts, which release cytotoxic factors. $CD4^+$ cells subsequently undergo apoptosis and are depleted from the 2nd to the 4th week of the disease in the affected lymph nodes. Apoptotic $CD4^+$ cells are then phagocytized by $CD163^+$, MPO^+, and $CD204^+$ macrophages.[14]

The number of peripheral blood monocytes was high in our cases (67.3%), and increased through the disease course. The proportion of $CD123^+$ cells (PDCs), $Mx1^+$ cells, and $CD8^+$ cells in the lymph node lesions showed a tendency similar to the peripheral blood monocytes from onset. However, the temporal change in $CD4^+$ cells in the lesions showed a very steep decrease from the 2nd to the 4th week, and then gradual increase afterward.

Table 3. Temporal change of number of $CD4^+$, $CD8^+$, $CD123^+$, and $Mx1^+$ cells in lesions and non-lesions tissue of lymph nodes, and peripheral blood monocytes.

Case number	Day	Mono (%)	Lesion (%)				Non-lesion (%)			
			CD123	CD4	CD8	Mx1	CD123	CD4	CD8	Mx1
1	4	5	1.4	35.9	17.9	51.8	0.9	29.9	8.3	2.8
2	6	7	2.0	54.1	5.7	17.9	3.3	44.9	7.5	2.4
Average	5.0	5.9	1.7	45.0	11.8	34.9	2.1	37.4	7.9	2.6
standard deviation	1.4	1.3	0.4	12.8	8.6	24.0	1.7	10.6	0.6	0.2
3	9	-	7.4	26.3	13.8	53.6	0.6	6.7	11.7	8.0
4	9	9	14.2	39.7	35.9	47.0	1.0	10.2	7.6	3.9
5	15	-	1.6	5.8	24.4	74.0	1.3	11.8	10.0	2.4
6	19	-	4.5	24.7	16.6	65.1	3.8	25.8	6.0	22.1
7	20	4	1.6	13.5	5.7	45.6	2.2	85.7	12.8	9.3
8	20	11	10.1	29.3	35.6	48.8	2.3	15.8	11.8	3.8
Average	15.3	8.0	6.6	23.2	22.0	55.7	1.9	26.0	10.0	8.2
standard deviation	5.2	3.6	5.0	12.0	12.2	11.4	1.1	30.0	2.7	7.3
9	32	9	7.6	33.4	46.4	65.5	2.8	49.7	15.4	12.1
10	37	9	3.1	25.2	16.5	57.2	0.1	17.4	7.7	6.6
11	37	-	3.4	35.4	41.3	52.5	1.8	23.6	5.3	8.3
12	49	8	17.8	24.5	19.8	58.9	6.6	39.8	28.6	11.8
13	50	8	2.7	26.8	27.1	72.4	1.6	19.7	19.0	14.9
14	54	9	17.2	50.5	24.7	66.7	0.8	19.1	4.0	6.9
15	55	11	17.2	48.6	28.9	71.1	6.4	22.0	8.4	2.5
Average	44.9	9.0	9.9	34.9	29.2	63.5	2.9	27.3	12.6	9.0
standard deviation	9.3	1.1	7.3	10.8	10.9	7.5	2.6	12.4	8.9	4.2
16	89	9	19.5	42.9	47.9	59.6	2.8	21.3	5.7	8.5
17	93	8	11.7	42.0	40.9	77.2	1.0	24.1	19.9	5.9
18	108	13	21.2	42.2	32.9	51.9	0.3	22.3	9.3	6.6
Average	96.7	10.1	17.5	42.3	40.6	62.9	1.4	22.5	11.6	7.0
standard deviation	10.0	2.5	5.1	0.5	7.5	13.0	1.3	1.4	7.4	1.3

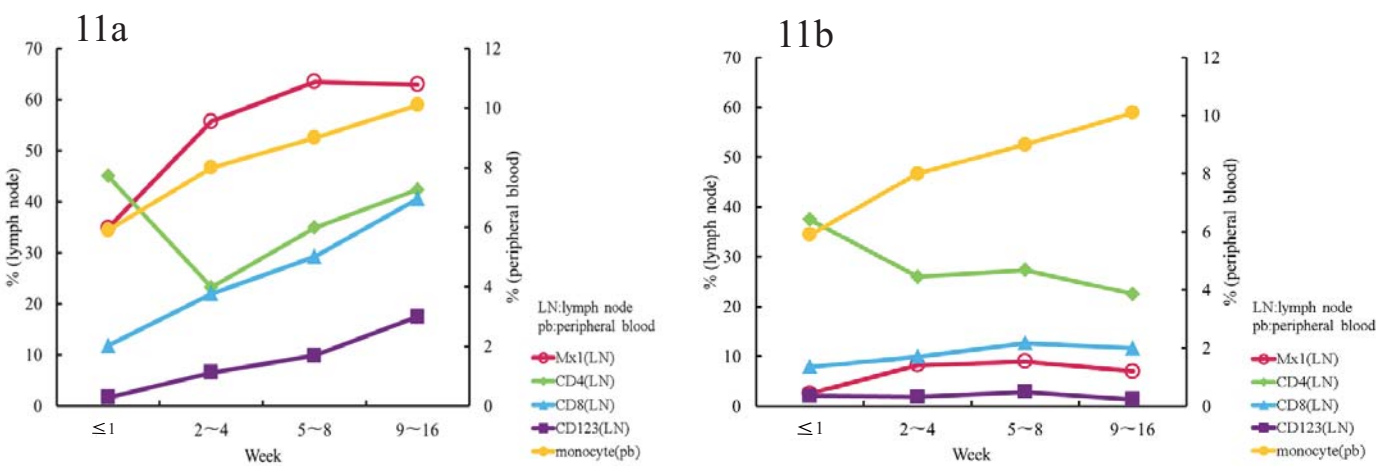

Fig. 11. Temporal changes in proportion of $CD4^+$, $CD8^+$, $CD123^+$ (plasmacytoid dendritic cells; PDCs), and $Mx1^+$ cells in the lymph node lesions, and peripheral blood monocytes. The number of peripheral blood monocytes, $CD8^+$ cells, PDCs, and $Mx1^+$ cells in the lymph node lesions gradually increases with time (*11a*). However, other than $CD4^+$ cells, no changes are detected in non-lesion tissues (*11b*).

On the other hand, in the non-lesion tissue of the lymph nodes, PDCs, $Mx1^+$ cells, and $CD8^+$ cells showed almost no temporal changes, but $CD4^+$ cells gradually decreased with time. After virus infection, $CD8^+$ cells may transform into immunoblasts, which release cytotoxic factors, and virus-affected $CD4^+$ cells become apoptotic and are phagocytized by macrophages.

PDCs are bone marrow-derived dendritic cells and differ from the lymphocytes and Langerhans cells.[17,18] After leaving the bone marrow, PDCs have been reported to migrate into the T cell area of lymph nodes via high endothelial venules.[18] In NEL, PDCs become larger and more irregular in lesions compared with those in the non-lesion tissue, and play important roles, including production of interferon (IFN)-α against virus infection, activation of $CD8^+$ cells to immunoblasts, induction of apoptosis of infected $CD4^+$ cells, elimination of apoptotic cells by macrophages, facilitation of $CD4^+$ cells activation and prevention of their exhaustion by apoptosis.[18-20] PDCs play specific roles, such as innate protection against cytopathic viruses and facilitation of adaptive immune response (Fig. 12). PDCs produce IFN-α, which induces expression of the marker Mx1. $Mx1^+$ cells mediate antiviral activity,[17] and were specifically detected in NEL in the present study, but not in the tonsils, tuberculosis, other reactive lymphadenitis, or malignant lymphoma (data not shown). The detection of $Mx1^+$ cells suggests the production of IFN-α in NEL, and may be highly useful for differential diagnosis for NEL.

The pathogenesis of the disease remains obscure, but may be associated with viral infection due to much clinicopathological evidence.[6,7,12,15,16,19,21,22] IFN-α produced by PDCs after persistent viral infection often induces common cold-like symptoms and systemic lupus erythematosus (SLE)-like syndrome, which is clinically similar to NEL.[17,19] Therefore, it is important to differentiate SLE from NEL.[4,23] In NEL, IFN-α is induced by viral nucleic acids within PDC endosomes, whereas it is induced by self-nucleic acids in SLE.[18] SLE shows a high $CD4^+/CD8^+$ cell ratio and a high degree of blastic transformation of peripheral blood lymphocyte by phytohemagglutinin, and a high titer of anti-DNA and anti-nuclear antibodies. However, in NEL, production of IFN-α is transient and mild, with a low degree of blastic transformation by phytohemagglutinin, and anti-DNA and anti-nuclear antibodies are rarely produced. The typical histological feature of lymph node involvement in SLE is coagulation necrosis, similar to that of the late stage of NEL.[14] Therefore, there are critical differences between these two disorders both clinicopathologically and pathogenically.[14] Furthermore, several other diseases must also be differentiated from NEL, including malignant lymphoma,[11,13] infectious mononucleosis,[14] and other lymphadenitis.[7,9,24,25]

In conclusion, PDCs inducing IFN-α play an important

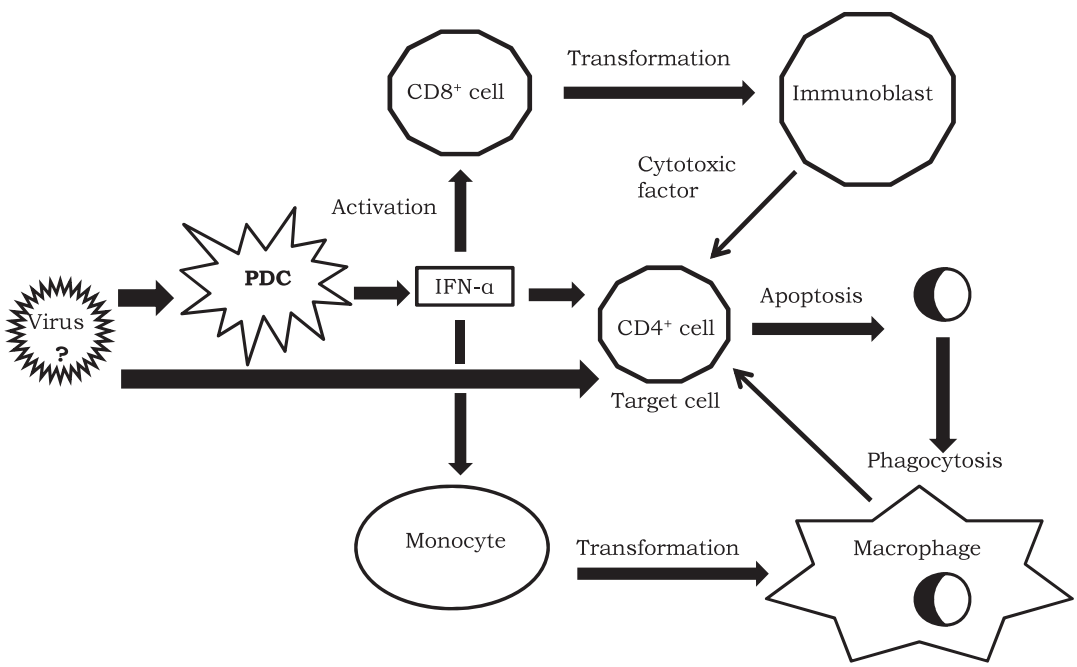

Fig. 12. Postulated pathway after infection in necrotizing lymphadenitis. Interferon-α production in response to viral infection induces $CD8^+$ cells, $CD4^+$ cells, and monocyte transformation to immunoblasts, apoptotic cells, and macrophages, respectively. Apoptotic cells are then phagocytized by macrophages. *PDC*, plasmacytoid dendritic cell; *IFN-α*, interferon-α

role in the regulation of immune activity against viral infections in necrotizing lymphadenitis.

CONFLICT OF INTEREST: The authors declare no conflict of interest.

REFERENCES

1 Fujimoto Y, KojimaY, Yamaguchi K: Cervical subacute necrotizing lymphadenitis. Int Med 30:920-927, 1972 (*in Japanese*)
2 Kikuchi M: Lymphadenitis showing focal reticulum cell hyperplasia with nuclear debris and phagocytes. A clinicopathological study. Acta Haem Jpn 35:379-380, 1972 (*in Japanese*)
3 Wakasa H, Kimura N: Lymphadenitis accompanying small necrotic focus. Trans Soc Pathol Jpn 62:138-139, 1973 (*in Japanese*)
4 Kuo TT: Kikuchi's disease (histiocytic necrotizing lymphadenitis). A clinicopathologic study of 79 cases with an analysis of histologic subtypes, immunohistology, and DNA ploidy. Am J Surg Pathol 19:798-809, 1995
5 Ali MH, Horton LW: Necrotizing lymphadenitis without granulocytic infiltration (Kikuchi's disease). J Clin Pathol 38:1252-1257, 1985
6 Pileri S, Kikuchi M, Helbron D, Lennert K: Histiocytic necrotizing lymphadenitis without granulocytic infiltration. Virchows Arch A Pathol Anat Histol 395:257-271, 1982
7 Feller AC, Lennert K, Stein H, Bruhn HD, Wuthe HH: Immunohistology and aetiology of histiocytic necrotizing lymphadenitis. Report of three instructive cases. Histopathology 7:825-839, 1983
8 Kikuchi M, Takeshita M, Tashiro K, Mitsui T, Eimoto T, *et al*.: Immunohistological study of histiocytic necrotizing lymphadenitis. Virchows Arch A Pathol Anat Histol 409:299-311, 1986
9 Carbone A, Manconi R, Volpe R, Poletti A, de Paoli P, *et al*.: Enzyme- and immunohistochemical study of a case of histiocytic necrotizing lymphadenitis. Virchows Arch A Pathol Anat Histol 408:637-647, 1986
10 Tsang WY, Chan JK, Ng CS: Kikuchi's lymphadenitis: A morphologic analysis of 75 cases with special reference to unusual features. Am J Surg Pathol 18:219-231, 1994
11 Rivano MT, Falini B, Stein H, Canino S, Ciani C, *et al*.: Histiocytic necrotizing lymphadenitis without granulocytic infiltration (Kikuchi's lymphadenitis). Morphological and immunohistochemical study of eight cases. Histopathology 11:1013-1027, 1987
12 Turner RR, Martin J, Dorfman RF: Necrotizing lymphadenitis. A study of 30 cases. Am J Surg Pathol 7:115-123, 1983
13 Chamulak GA, Brynes RK, Nathwani BN: Kikuchi-Fujimoto disease mimicking malignant lymphoma. Am J Surg Pathol 14:514-523, 1990
14 Asano S, Mori K, Yamazami K, Sata T, Kurata A, *et al*.: Necrotizing lymphadenitis (NEL) is a systemic disease characterized by blastic transformation of $CD8^+$ cells and apoptosis of $CD4^+$ cells. Virchows Arch 464:95-103, 2014
15 Asano S, Akaike Y, Muramatsu T, Wakasa H, Yoshida H, *et al*.: Necrotizing lymphadenitis. A clinicopathological and immunohistological study of four familial cases and five recurrent cases. Virchows Arch A Pathol Anat Histopathol 418:215-223, 1991
16 Asano S, Kanno H, Tominaga K, Muramatsu T, Nozawa Y, *et al*.: Necrotizing lymphadenitis. Electron microscopical and immunohistochemical study. Acta Pathol Jpn 37:1071-1084, 1987
17 Farkas L, Beiske K, Lund-Johansen F, Brandtzaeg P, Jahnsen FL: Plasmacytoid dendritic cells (natural interferon-α/β-producing cells) accumulate in cutaneous lupus erythematosus lesions. Am J Pathol 159:237-243, 2001
18 Tang F, Du Q, Liu Y-J: Plasmacytoid dendritic cells in antiviral immunity and autoimmunity. Sci China Life Sci 53:172-182, 2010
19 Cervantes-Barraguan L, Lewis KL, Firner S, Thiel V, Hugues S, *et al*.: Plasmacytoid dendritic cells control T-cell response to chronic viral infection. Proc Natl Acad Sci U S A 109:3012-3017, 2012
20 Pilichowska ME, Pinkus JL, Pinkus GL: Histiocytic necrotizing lympadenitis (Kikuchi-Fujimoto Disease): Lesional cells exhibit an immature dendritic cell phenotype. Am J Clin Pathol 131:174-182, 2009
21 Asano S, Muramatsu T, Kanno H, Wakasa H: Dermatopathic lymphadenopathy. Electronmicroscopic, enzyme-histochemical and immunohistochemical study. Acta Pathol Jap 37:887-900, 1987
22 Imamura M, Ueno H, Matsuura A, Kamiya H, Suzuki T, *et al*.: An ultrastructural study of subacute necrotizing lymphadenitis. Am J Pathol 107:292-299, 1982
23 Kojima M, Nakamura S, Itoh H, Yoshida K, Suchi T, *et al*.: Lymph node necrosis in systemic lupus erythematosus. A histopathological and immunohistochemical study of four cases. APMIS 109:141-146, 2001
24 Asano S: Granulomatous lymphadenitis. J Clin Exp Hematop 52:1-16, 2012
25 Nieman RB: Diagnosis of Kikuchi's disease. Lancet 335:295, 1990